Journal of Materials Chemistry B

Accepted Manuscript

ROYAL SOCIETY OF CHEMISTRY

www.rsc.org/materialsB

Synthesis of Aqueous AgInS/ZnS@PEI as Self-Indicating Nonviral Vector for Plasmid DNA Self-Tracking Delivery

Wentao Yang[a,§], *Weisheng Guo*[b,§], *Tingbin Zhang*[b], *Weitao Yang*[a], *Lin Su*[a], *Lei Fang*[a], *Hanjie Wang*[a], *Xiaoqun Gong**[a], *and Jin Chang**[a,c,d]

a School of Materials Science and Engineering, School of Life Sciences, Tianjin University, Tianjin 300072, China

b CAS Key Laboratory for Biological Effects of Nanomaterials & Nanosafety National Center for Nanoscience and Technology, Beijing , 100190 , China

c Tianjin Engineering Center of Micro-Nano Biomaterials and Detection-Treatment Technology, Tianjin 300072, China

d Collaborative Innovation Center of Chemical Science and Engineering (Tianjin), Tianjin 300072, China

§ W.Y. and W.G. have equal contribution to this paper.

Corresponding Authors

*Jin Chang: Email: jinchang@tju.edu.cn. Tel: +86-22-27401821

*Xiaoqun Gong: Email: gongxiaoqun@tju.edu.cn.

ABSTRACT:

Various nanoparticles have been employed for gene delivery. Revealing the endocytosis or phagocytosis behaviors of the gene delivery system is critical for designing of sophisticated gene therapies. Herein, a kind of water-soluble PEI capped AgInS/ZnS (ZAIS@PEI) quantum dots were synthesized as self-indicating gene vectors in the presence of branched polyethylenimine (PEI) and mercaptopropionic acid (MPA). The as-prepared ZAIS@PEI QDs could efficiently condense plasmid DNA into nanocomplexes with strong fluorescence, which can reveal their positions during the gene transfection. Our results confirmed that the ZAIS@PEI could mediate plasmid DNA into Hela cells with high transfection efficiency of 40% and low cytotoxicity, meanwhile allowing real-time monitoring the gene transfection. The obtained ZAIS@PEI QDs were verified as versatile self-tracking gene vectors, which integrated gene delivery with bioimaging functions without external labeling.

Keywords: AgInS; Quantum dots; Self-indicating, Gene transfection

1. Introduction

Gene therapy technology is a promising therapeutic approach due to its unique advantage that could delivery specific gene to different disease.[1-2] A gene delivery vehicle is of essential importance to have the gene of interest delivered to targeted cells efficiently which usually cannot be achieved by naked gene.[3-5] Although viral vectors are currently the most efficient gene transfer agents,[6] the overall safety of viral vectors is controversial.[7] Alternatively, polymeric gene delivery systems such as

polyethylenimine (PEI) have been intensely studied as promising gene delivery vehicle candidates, which could achieve pretty high transfection efficiency as positive transfection agents.[8-9] Since the study on polymeric gene vectors is still on the way and the delivery mechanism is yet unclear, the polymeric gene vectors are usually labeled with kinds of fluorophors to visualize their intracellular delivery pathway. For example, prior to condensing negative-charged DNA, some polymeric gene vectors were conjugated with some fluorescein (FITC, Cy-5 etc), enabling them could be detected and located by fluorescence signals. However, there are some concerns about this fluorescent tagging strategy. First, the physicochemical properties of the polymeric vectors could be changed when modified with fluorescein. Second, the labeled vectors may behave differently from the untagged ones during endocytosis or phagocytosis. Third, during the phagocytic process, the coupled fluorescent moiety might dissociate from the polymeric vector/DNA-fluorescein conjugate, leading to mismatch in locations between polymeric vector and fluorescein. Therefore, it's urgently necessary to develop a kind of self-fluorescent label-free gene vectors with high gene transfection efficiency and low toxicity.

Compared with fluoresceins, quantum dots (QDs) have gained more intense attentions and been widely used for bio-imaging and bio-labeling, benefiting from their excellent photochemical properties, including higher fluorescence intensity, tunable emission photoluminescence, broad excitation spectra and high resistance to photobleaching.[10-14] While QDs are excellent biological fluorescent probes, they are also can be used as effective delivery vehicles for several therapeutic biomolecules

such as drug, gene and so on.[15-19] For instance, Mao and co-workers proposed a kind of L-arginine-functional-modified CdSe/ZnSe QDs, which achieved the simultaneous tracking as well as the delivery of small interfering RNA (siRNA) to selectively silence HPV18 E6 gene in HeLa cells.[15] However, the toxicity originating from CdSe-based QDs is a great drawback for their further biomedical applications. As an emerging alternate, AgInS-based QDs are of particular interests for biomedical applications due to the advantage of containing no toxicity elements (Cd, Pb and Hg). For example, Zhang and co-workers have successfully synthesized AgInS nanocrystals with excellent biocompatibility for passive targeted delivery to the tumor site, and low cytotoxicity of the nanocrystals was also demonstrated via histological analysis.[20]

Inspired by the above issues, we set out to develop a kind of AgInS QDs capped with PEI as self-indicating visible non-viral gene delivery system. As showed in scheme 1, the PEI-capped AgInS/ZnS (ZAIS@PEI) QDs were synthesized in aqueous solution with PEI and mercaptopropionic acid (MPA) as surface stabilizer. The PEI on the surface of the QDs as cationic polymers offered the functional groups aminos, which made the QDs positive charged and directly interact with gene without further surface modification. Thus, the as-prepared ZAIS@PEI QDs could serve as vectors to deliver gene and track the genetic intracellular delivery pathway by self-fluorescence. Moreover, the presence of negatively charged MPA decreased the electropositive density on the surface of the QDs, endowing the gene vector with high gene transfection efficiency (40%) as well as low toxicity.

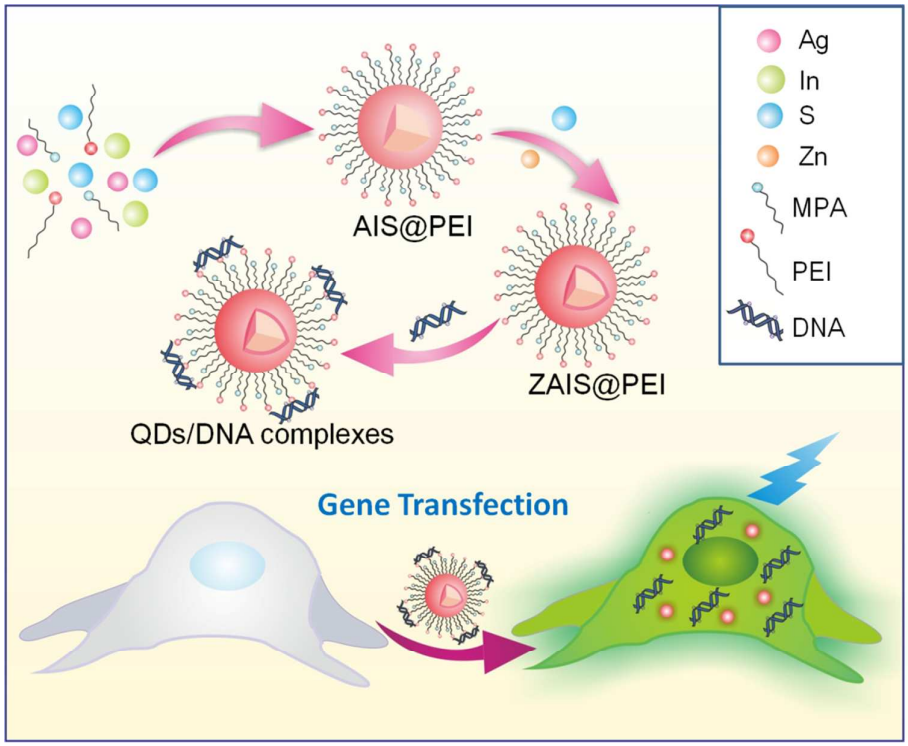

Scheme 1 Schematic illustration of the synthesis and cellular labeling process of ZAIS@PEI QDs

2. Materials and Methods

2.1 Materials and Chemicals.

Silver (I) nitrate ($AgNO_3$, 99.9%), indium (III) nitrate hydrate ($In(NO_3)_3 \cdot xH_2O$ 99.99%), zinc (II) nitrate hydrate ($Zn(NO_3)_2 \cdot 6H_2O$, 99%), sodium hydroxide (NaOH, 96.0%), sodium citrate (99%), sodium sulfide hydrate ($Na_2S \cdot 9H_2O$, 98.0%), poly(ethylene imine) (PEI 10 KDa and PEI 25 KDa), 3-mercaptopropionic acid (MPA, 98%) and fluorescein (99%) were purchased from Sigma-Aldrich (St. Louis, MO, USA). All Chemicals were used without further purification. Double distilled water was prepared using GFLM-2302 water distiller.

2.2 Synthesis of ZAIS@PEI QDs.

The synthesis of ZAIS@PEI QDs was developed from the previous reported method.[21] 25mL of aqueous solution containing 0.1 mmol $AgNO_3$, 0.4 mmol $In(NO_3)_3$, 0.03 mmol PEI and 0.2 mmol MPA was prepared in a 50 mL flask under ambient conditions. 3 mL of Na_2S (0.2 M) solution was swiftly injected into the above mixture solution at 95 ^oC under magnetic stirring. The resulting mixture was kept boiling for 1 h to allow growth of ZAIS@PEI QDs. Then, a 4 mL aqueous solution containing 1 mmol $Zn(NO_3)_2$ and 1.25 mmol sodium citrate was slowly added into the mixture. Subsequently, 2 mL aqueous solution containing 1 mmol Na_2S was dropwise added into the mixture. The last two steps took about 30 min. The reaction mixture was continuously refluxed for another 1 h at 95 ^oC. After cooling down to room temperature, the equal amount of ethanol was added to precipitate the resulting QDs. The obtained precipitate was redispersed in 4 mL water. This procedure repeated twice to remove the excess salts. The purified QDs were resuspended in water and stored at 4^oC. For comparison, ZAIS@PEI QDs with different emission color were prepared by varying the ratio of the ligand combinations.

2.3 Preparation of vector/DNA complexes.

ZAIS@PEI QDs, PEI 10 KDa, PEI 25 KDa and green fluorescence protein (GFP) plasmid DNA were separately dissolved in double distilled water and the solutions were filtered with 0.22 mm sterile filters. Vector/DNA complexes at varied ratios were then formulated by adding vector of desired concentrations to an equal volume of a defined DNA solution, pipetting up and down to make the mixture homogeneously

mixed. The mixtures were incubated at room temperature for 30 min to allow complex formation. In this study, the complexing ratio was expressed as the weight ratio of vector/DNA.

2.4 Agarose gel electrophoresis.

The vector/pDNA complexes at different weight ratios were prepared freshly as described above. 10 μL of complex solution was mixed with a loading buffer, and loaded into 1% agarose gel containing GoldView I (0.5 mg/ml). The electrophoresis experiment was performed for 20 min in TAE buffer (1X) at 100 V, and the image was captured through BioImaging Systems(UVP).

2.5 Cytotoxicity evaluation by MTT assay.

Hela cells were cultured in Dulbecco's modified Eagle's medium (DMEM) with 10% fetal bovine serum and 1% penicillin/streptomycin. The cells were placed in a 96-well microplate at a density of 10^4 cells in 200 μL of complete DMEM culture medium, and incubated overnight at 37 ^{o}C with 5% CO_2 humidified atmosphere. Then, the medium was replaced by fresh DMEM with different concentration of ZAIS QDs (25, 50, 75, 100 and 200 μg/mL), 5 duplicates were obtained for each concentration. After incubation for 24 h, 10 μL of 1-methyltetrazole-5-thiol (MTT, 5 mg/mL) was added to each well, followed by incubating for 4 h to allow the formation of formazan crystals. The medium was then removed by aspiration, and 200 μL of dimethyl sulfoxide (DMSO) was placed to dissolve the purple formazan crystals. Absorbance was measured at 570 nm. The relative cell viability was evaluated by normalizing with the results acquired with no QD-loading.

2.6 Hemolysis assay.

Blood was obtained from healthy volunteers in sterile lithium heparin vacutainers (signed consent forms were obtained from the volunteers before blood collection). The study protocol was in accordance with the ethical standards of the 1964 Declaration of Helsinki and its later amendments, and approved by the ethics committee of the second hospital of Tianjin medical university. Red blood cells (RBCs) were separated by centrifugation from 5 mL of whole blood diluted in 0.9% saline solution at 1500 rpm for 10 min. The supernatant containing plasma and platelets was removed. Washing the precipitate until the supernatant was clear. The RBC pellet was resuspended in 50 mL saline solution. The as-prepared ZAIS@PEI QDs and PEI polycations samples were diluted to a required concentration in cell suspension. The samples incubated for 3 h at 37 ^{o}C in the incubator. Positive and negative controls were produced by adding cell suspension to the distilled water and saline, respectively. After incubation, the mixtures were centrifuged with high speed (20000 rpm for 30 min) to remove the vectors and cells. The optical density of the supernatant was measured at 545 nm. The percentage of hemolysis was calculated as follows:

$$\%\text{hemolysis} = \left[\frac{\text{ODtest} - \text{ODneg}}{\text{ODpos} - \text{ODneg}}\right] * 100,$$

Where ODtest, ODneg, and ODpos are the absorbance values of the test sample, negative control (saline) and positive control (water), respectively. All the hemolysis

experiments were done in triplicate. For the observation of morphological changes of treated blood cells at the early stages of hemolysis, the cell pellet obtained after centrifugation was diluted in 0.9% saline solution, mounted on clean glass slides covered with cover slips, and observed under an Olympus BX41 microscope.

2.7 In vitro transfection and cell imaging.

Hela cells were cultured in 24-well plates at a density of $5*10^4$ cells per well and incubated for 12 h at 37 ^oC in 5% CO_2 humidified atmosphere. Before transfection the cell culture medium was replaced with 450 μL serum-free DMEM. 50 μL of vector/DNA complexes (containing 1 μg DNA) at various weight ratios prepared as described above were then added to each well. After incubating at 37 ^oC in 5% CO_2 for 12 h, the culture medium was replaced with 500 μL of complete medium, and then the cells were incubated for an additional 60 h. Transfection tests were performed in triplicate. After that, the cells were washed with PBS twice for imaging.

For tracking the gene vector transfection pathway, Lysosome Tracker Green DND (Invitrogen) was chosen for lysosome staining. First, 1μg/mL Lysosome Tracker stock solutions was prepared and added into the cell containing wells prior to the confocal microscope imaging. After incubation for 15 min, the cells were washed with PBS for 3 times and then imaged with laser confocal fluorescence microscope.

Characterization.

Ultraviolet-visible absorption spectra of QDs were obtained with a Shimadzu UV-2450 spectrophotometer at room temperature. Fluorescence spectra were recorded

on a Gangdong F-280 spectrofluorometer. The fluorescence quantum yield (QY) of QDs was valuated from the integrated fluorescence intensities of the QDs and the reference (Rhodamin 6G QY=95% at 470 nm excitation). The QD samples for spectral measurement were all diluted to yield an absorbance of 0.05 at the excition wavelength.[14, 22-23] The QY of the samples was calculated using the following equation,

$$QYs = \frac{Fs * Ar * QYr}{Fr * As},$$

Where F is the integrated fluorescence emission, A is the absorbance at the excitation wavelength, and the subscripts s and r refer to the sample and the reference, respectively. Transmission electron microscopy (TEM) images were taken using Tecnai G2 F20 instrument operated at 200 kV, which is equipped with an energy-dispersive X-ray (EDX) detector using for elemental analysis. X-ray diffraction (XRD) patterns were acquired on a Rigaku Ultima III diffractometer equipped with a rotating anode and a Cu-Ka radiation source. Fluorescence images of HeLa cells were obtained using an Olympus FV1000-MPE multiphoton laser scanning confocal microscope (Japan). The dispersion property of the QDs in solution was taken using a particle size analyzer (Nano ZS, Malvern).

3. Results and Discussion

3.1 Characterization of ZAIS@PEI quantum dots.

In this work, we explored the synthesis of the water-soluble ZAIS@PEI QDs in aqueous phase at varied precursor ratios. Compared to the traditional organic-phase

synthetic method, this procedure is simple, low-cost and environmentally friendly. Figure 1A showed normalized PL spectra ZAIS QDs with variable molar ratios of Ag/In. The emission peaks had tunable maximum intensity of wavelength ranging from 557 nm to 715 nm when varying the molar ratio of Ag/In from 1/12 to 1/1. The blue-shift of the emission maximum wavelength with increasing Ag deficiency resulted from the widening of energy gap, which was consistent with current literature reports.[21, 24-25] The valence bandgap maximum of ZAIS@PEI consisted of orbitals of S 3p and Ag 4d, decreasing the content of Ag reduced the valence band maximum, thus widening the bandgap. The corresponding digital image of the ZAIS@PEI QDs prepared with different Ag/In ratios was shown in Figure 1B, which was taken under the ultraviolet light. Aliquots of the reaction solution were sampled at 5, 10, 15, 30, 60 and 75 min at 95 ^{o}C. The PL emission and absorption spectra of the AIS QDs as a function of time was shown in Figure S1 (see Supporting Information). Very weak but broad emission peak was observed at 570 nm after 5 min injection of sulfur precursor, and shifted to 590 nm with significant improvement of PL intensity after 75 min. This was owed to a size increase with growth time. There was not any well-defined exciton absorption peaks in the absorption spectra showed in Figure S1B (see Supporting Information), and large Stokes shift was observed between the absorption onset and the PL peak. These features maybe caused by the defect-based donor-acceptor pair recombination rather than excitonic emission.[26-28] A high photolumiscence quantum yield (QY) is necessary for bioimaging. Our results revealed that the QY values of the as-prepared ZAIS@PEI QDs were ranging from 10% to 25% (Figure S2), which was

competent to the further use in biological area.[29]

The TEM image of the as-prepared ZAIS QDs was displayed in Figure 1D. The QDs were quasi-spherical particles with an average diameter of about 4 nm. The high-resolution TEM image in Figure S3A (see Supporting Information) showed the well-resolved lattice planes, which demonstrated the good crystallinity of the QDs. Energy dispersive X-ray spectroscopy (EDX) shown in Figure S3B (see Supporting Information) confirmed the presence of the elements: Ag, In and S. The XRD pattern shown in Figure 1C revealed that both the as-prepared AIS and ZAIS QDs adopted the tetragonal chalcopyrite crystal structure.[30] The significant improvement of and increased 2θ values of diffraction peaks were observed on modification with ZnS, confirming the formation of ZAIS alloy.[31]

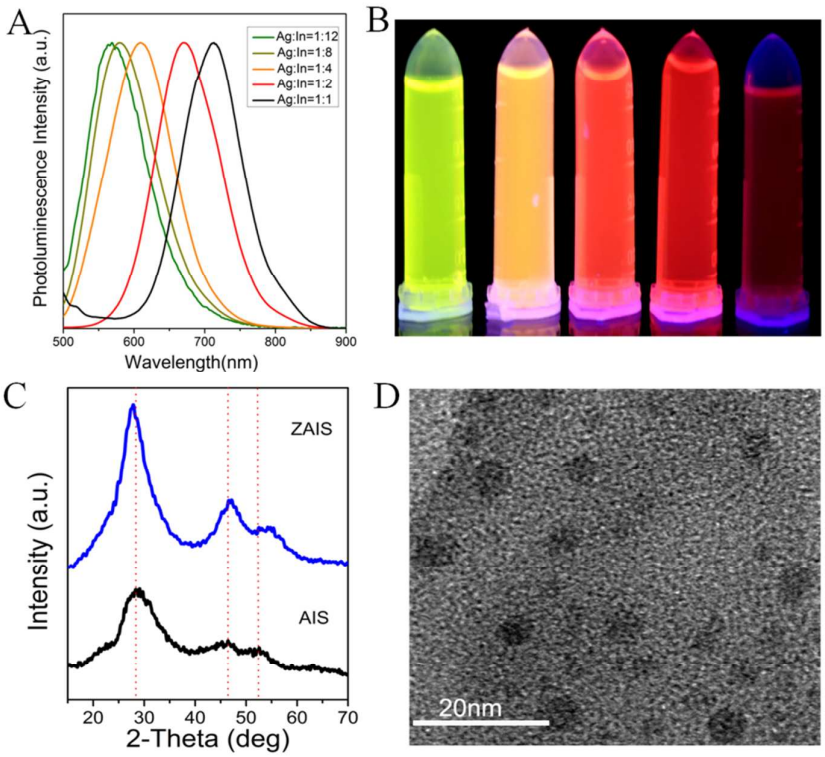

Figure 1. Photoluminescence spectra (A) and digital pictures under UV-light (B) of

the ZAIS@PEI QDs with different Ag/In ratios; (C) XRD profile of AIS@PEI and ZAIS@PEI QDs; (D) TEM images of ZAIS@PEI QDs

The colloidal stability of the as-prepared ZAIS@PEI QDs in different chemical environment was also examined. Same amount of ZAIS@PEI QDs samples were dispersed in water with different pH values and NaCl concentrations. Their effective particle sizes and PL intensity were measured after 8 h incubation. As shown in Figure 2A, there's no obvious change on the effective particle size and PL intensity of each ZAIS@PEI QDs sample with the increasing salt concentration from 0 to 2 M, and the corresponding photograph was presented in Figure 2B. The results demonstrated that the as-prepared ZAIS@PEI QDs could be well-dispersed in the NaCl solutions with concentration as high as 2 M. The PL intensity could maintain unchanged with the pH value range, which was shown in Figure 2C, the corresponding digital pictures were displayed in Figure 2D. This revealed that the QDs possessed high level of tolerance of pH values ranging from 4 to 10.5. This impressive colloidal stability may be attributed to the interaction of MPA and PEI, where the coexistence of carboxyl and amino groups forms the buffer system, resulting to the high tolerance in different chemical environment.[32] These results suggested that the ZAIS@PEI QDs were promising candidates for gene vectors.

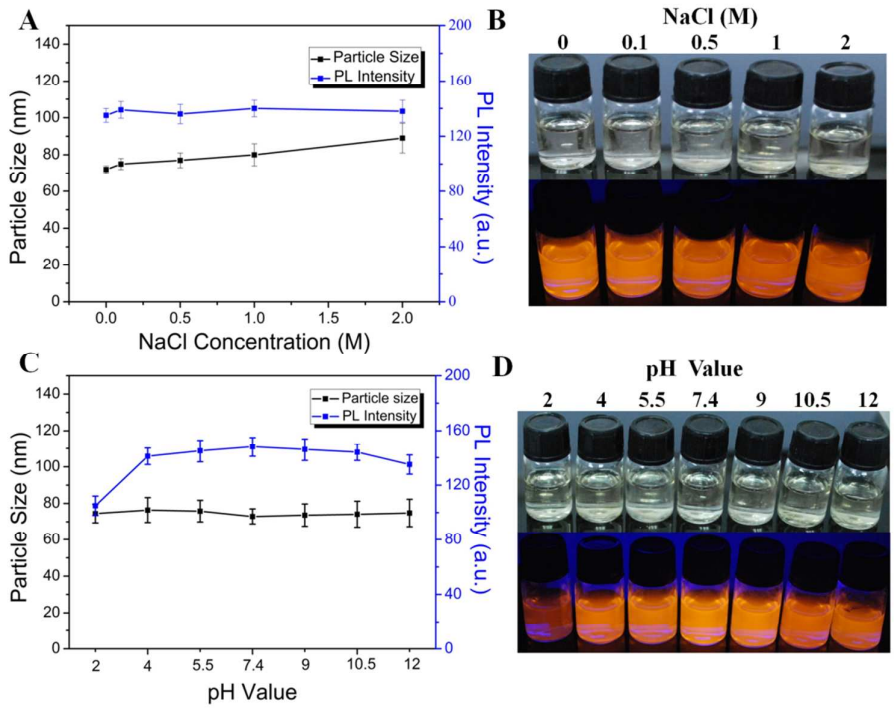

Figure 2. Colloidal stability of as-prepared ZAIS@PEI QDs (A. the effective particle size and PL intensity in aqueous solution with different NaCl concentration; B. the corresponding photographs of QDs dispersed in water with different NaCl concentration; C. the effective particle size and PL intensity in aqueous solution with different pH values; D. the corresponding photographs of QDs dispersed in water with different pH values).

3.2 Formation of QDs/DNA complexes.

It is of great significance to form a stable complex between a vector and DNA for efficient gene delivery. Figure 3 displayed the agarose gel electrophoresis patterns of the QDs/DNA complexes at weight ratios ranging from 0.5 to 8. It was shown that the QDs could completely retard pDNA at the ratio of 1, which could indicate that the QDs were capable of condensing DNA efficiently at a proper ratio. The retard capability of the PEI-capped QDs was below the PEI 10 KDa (shown in Figure 3A),

this was owing to the negatively charged group COO- in the ligand of MPA counteract the positive charges of PEI on the QDs surface, resulting in a reduction of positive charge density. Nevertheless, the retard capability of the PEI-capped QDs was similar to the PEI 25 KDa (Figure 3B), this could prove that the ZAIS@PEI QDs had excellent ability to condense DNA. With the increasing weight ratio of QDs/DNA, the zeta potentials of the QDs/DNA complexes were increased, and the particle sizes were decreased at the same time, which was shown in Figure 4A. We found that the particle size of the complexes was heavily increased when the ratio of QDs/DNA was 3/1, this was due to the QDs/DNA complexes were nearly electrically neutral (Figure 4B) and had little mutual repulsive, which leaded to the accumulation of different complexes and the huge particle size. The formed complexes were positively charged with the ratio of QDs/DNA greater than 3/1, and the electrostatic interaction made the complexes well-dispersed, resulting in the small particle size of the QDs/DNA complexes. When the weight ratio was fixed at 5/1, the particle size of the formed complexes was around 200 nm, and the surface was slightly positive charged, which is in favor of the transmembrane behavior as well as low cytotoxicity. Therefore, the weight ratio of the QDs/DNA was fixed at 5/1 as the optimum ratio for transfection assay.

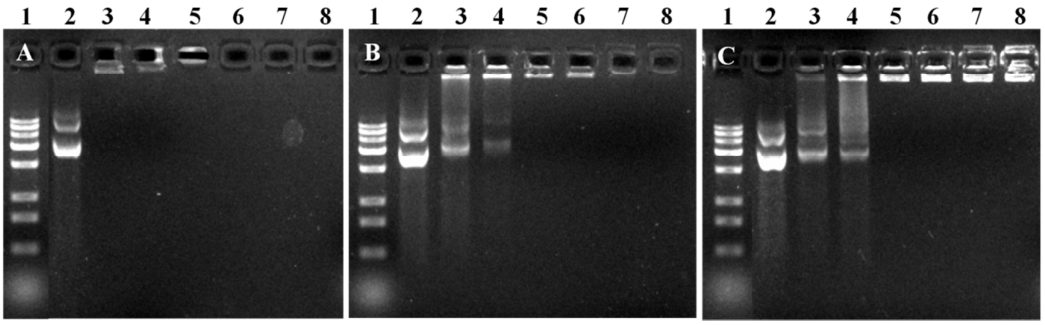

Figure 3. Electrophoresis patterns of Vectors/pDNA. (Vector A: PEI 10KDa ; Vector B: PEI 25KDa; Vector C: PEI-capped QDs. Lane1: 2 kb DNA ladder; lane2: plasmid DNA; lane3–8 represent the complexes with the weight ratios (vector/DNA) of 0.5, 0.8, 1, 3, 5 and 8, respectively.)

3.3 Cytotoxicity Tests and Hemolysis Assay

Aimed at simultaneous bioimaging and transfection ability, the ZAIS@PEI QDs need to have great optical properties and low cytotoxicity as well. To assess the cytotoxicity of the ZAIS@PEI QDs, we adopt a standard cell viability assay based on 1-methyltetrazole-5-thiol (MTT). As shown in Figure 5A, the cell viability of Hela cells is lightly decreased with the raising concentration of QDs. More than 85% of Hela cells were viable even at a concentration of 50 μg/mL, it was much higher than that of the PEI 10 KDa and PEI 25 KDa with less than 60% of cells viability. The results suggested that the as-prepared QDs remarkably reduced the cytotoxicity of the polycation of PEI. With the ligand of negative MPA incorporated on the surface of the QDs, the positive charge density of the polycation on the QDs surface was heavily reduced, which was ascribed to the low cytotoxicity of as-prepared QDs.[33] Moreover, the above gene transfection of the QDs was performed under the concentration of 50

μg/mL and the cells remained highly viable over the selected range, which was optimal for the transfection activity.

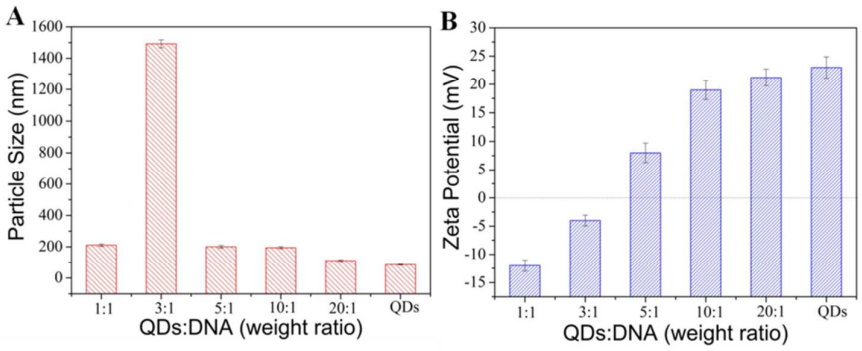

Figure 4. Particle size and Zeta potential of QDs/DNA complexes with varying ratios.

The hemocompatibility is of great importance before the materials can be used for in vivo applications, especially for materials required to contact blood. Figure 5B showed the hemolytic behaviors of ZAIS@PEI QDs and control groups (PEI 10 KDa and PEI 25KDa) at different concentrations (25, 50, 100 and 200 μg/mL). The ZAIS@PEI QDs exhibited much lower hemolysis degrees than the pristine PEI samples at same concentrations. The hemolysis rate of the QDs was below 4%, comparing to the high hemolysis degrees of the pristine PEI samples (over 20%). It was reported that up to 5% hemolysis was permissible for biomaterials.[34] In this regard, the as-prepared QDs are suitable as biomaterials. The observation of morphologically aberrant forms of RBCs was shown in Figure 5C. In presence of the ZAIS@PEI QDs, the RBCs appeared in a normal biconcave shape, which is consistent with the RBC immersed in saline. However, the exposure to the PEI 10KDa and PEI 25KDa samples induced the appearance of morphological aberrant

forms, just like the RBC immersed in water. This result confirmed the hemolysis degree measured in Figure 5B. Based on these results, the as-prepared QDs have good hemocompatibility and can be further applied to biomedical area with little hemolysis.

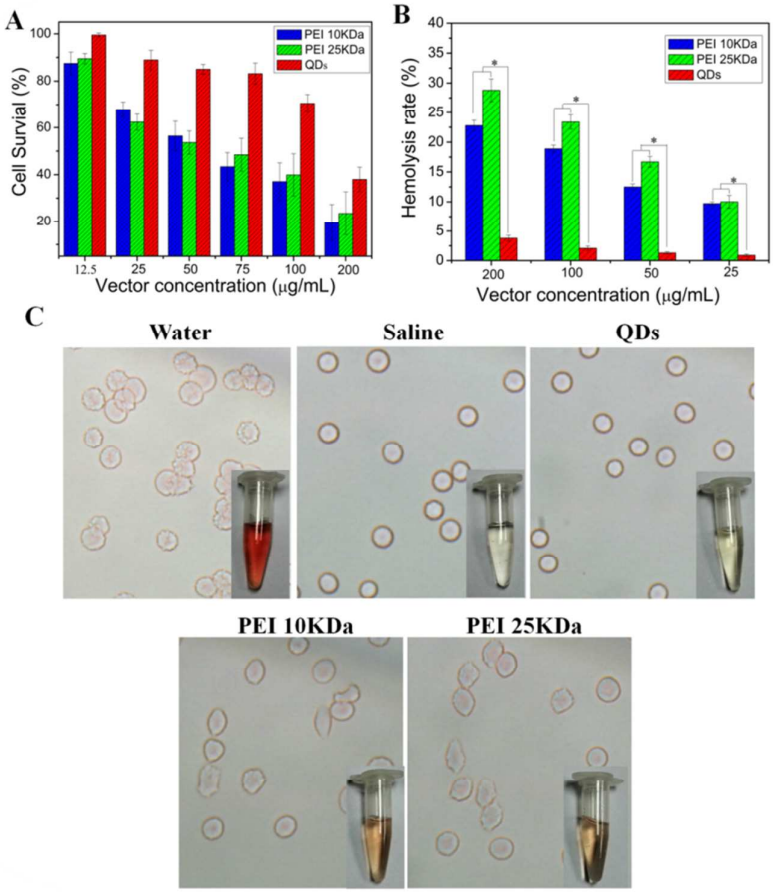

Figure 5. (A) Cytotoxicity test results from a MTT assay with different vector concentrations. (The values represent percentage cell survival.) (B) Hemolysis test results of gene vectors at different concentrations. (Statistical significance was calculated using the ANOVA method and is indicated by (*) for $p < 0.05$) (C) Red blood cell (RBC) hemolysis protection assay of the vectors at the concentration of 200 μg/mL, with positive control (water) and negative control (saline).

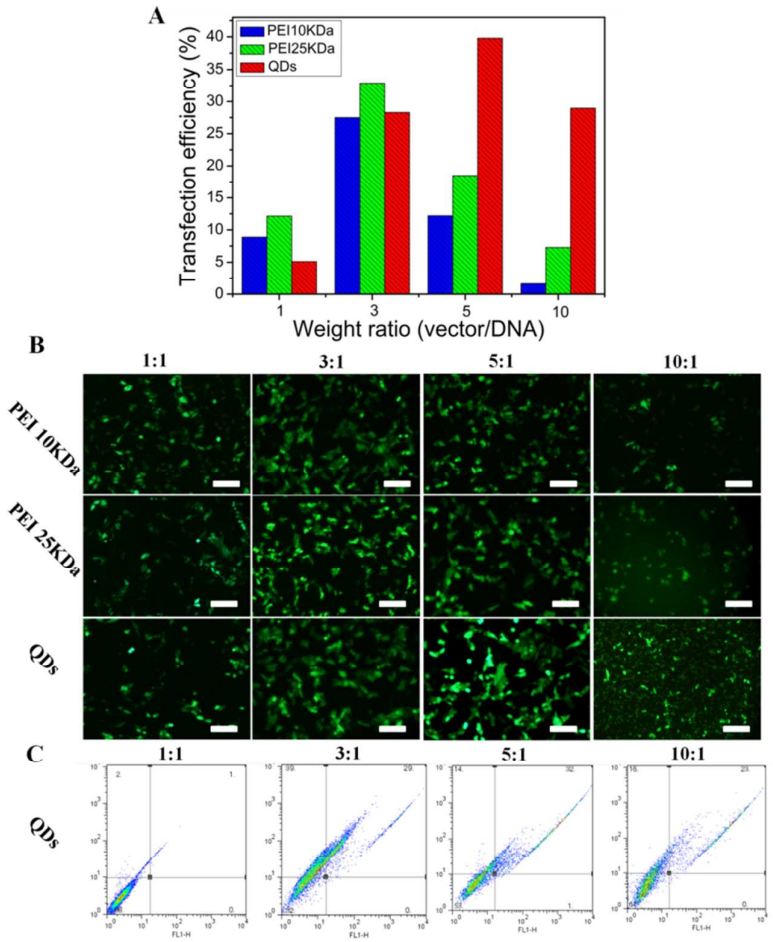

Figure 6. (A) Transfection efficiency with different Vector/DNA at varied weight ratios. (B) The corresponding images under blue-light after transfection with different Vector/DNA at varied weight ratios. (Scale bar:100 μm.)(C) The corresponding flow cytometric analysis after transfection with different Vector/DNA at varied weight ratios.

3.4 In vitro transfection and intracellular tracking of QDs/DNA complexes.

In this work, green fluorescent protein (GFP) gene was used to assess the in vitro gene transfection efficiency of the QDs/DNA complexes in Hela cells. We measured the transfection efficiency of QDs/DNA in comparison with those of PEI 10 KDa and PEI 25 KDa at various weight ratios by FCM. The transfection on Hela cells was

measured at 72 h after transfection by FCM. As shown in Figure 6A, the transfection efficiency of QDs was inferior to that of PEI 10 KDa and PEI 25 KDa when the ratio of vector/DNA was below 5/1, which was ascribed to the deficiency of the delivery vector of QDs. With the ratio increasing, the amount of delivery vector was adequate, thus the transfection efficiency of QDs was greatly improved and superior to the two kinds of PEI. The transfection efficiency of the ZAIS@PEI QDs came to the highest level of 40% when the ratio was fixed at 5/1. As discussed above, the QDs/DNA complexes with the ratio of 5/1 had proper particle size and weak positive charge, which was in favor of easy cross the cell membrane as well as low cytotoxicity. With increasing content of vector, the high intensity of polycation deteriorated the environment of the cells and damages the transfection efficiency. The negative charged group of MPA on the QDs surface could reduce the positive charge, and the more content of QDs could condense more DNA, which facilitated higher transfection efficiency for QDs. Furthermore, the transfection activity of both PEIs decreased markedly when the PEI/DNA weight ratio was higher than 5/1, which was ascribed to the cytotoxicity caused by the excess PEI ploycations. In addition to Hela cell, the gene transfection ability of the ZAIS@PEI QDs were also evaluated on 293T cells. As shown in Figure S6 (see Supporting Information), when the ratio of QDs/DNA was fixed at 5/1, the transfection efficiency reached a maximum of 32% after 48 h incubation post transfection.

The corresponding images taken under blue-light after transfection with different vector/DNA weight ratios were exhibited in Figure 6B. There was weak green

fluorescence in the pictures when the vector/DNA ratio was 1/1. With the content of vector increasing, the green fluorescence in the pictures got brighter and more concentrated. The brightness of green fluorescence reached the highest value when the weight ratio of QDs/DNA was 5/1, which agreed with the result measured by FCM. When the ratio of QDs/DNA was 10:1, there remained some green fluorescence of the cells, while there were only very few bright cells in the presence of PEI 10 KDa and PEI 25 KDa as vector, due to the high cytotoxicity of PEI polycations. The corresponding transfection results with different QDs/DNA ratios from flow cytometric analysis (Figure 6C) further demonstrated that the weight ratio 5/1 of the QDs/DNA was the optimum ratio.

Here we found an interesting phenomenon that the transfection with QDs/DNA complexes needed long time incubation (shown in Figure 7), and the highest transfection efficiency was realized with 72 h incubation after transfection. After 24 h incubation post transfection, little green fluorescence of GFP in the cells was observed under blue-light, but much more red fluorescence of QDs was observed under the green-light. With incubation prolonging up to 72 h, much more green fluorescence could be observed. In the case of PEI as vectors, high green fluorescence of the cells was appeared as early as 24h incubation after transfection (Seen in Figure S4 and Figure S5) (see Supporting Information). This may attribute to that the presence of MPA on the QDs surface decreases the buffering capacity of the vector, resulting slower escape of complexes from the endosomes, however, it did not directly correlate with the gene transfer ability.[32, 35] At the same time, the red fluorescence of QDs was

clearly observed all the time, thus we could trace the cells without other marker. This evidenced the successful integration of gene delivery and bioimaging functions in one single ZAIS@PEI QDs. Furthermore, we can make it possible that processes the visual treatment of gene therapy by simply using the as-prepared QDs as gene vector.

For the insight into the process of transfection, the cell internalization dynamics of the QDs/DNA complexes uptake, endocytosed into lysosome and endosomal escape were elucidated by establishing the degree of fluorescence colocalization of the QD signals with lysosome tracker in Hela cells.[36] As shown in Figure 8, the lysosome was marked with green fluorescence originating from the lysosome tracker, while ZAIS/PEI QDs intrinsically produced red fluorescence emission. After 4 h of incubation, whereas plenty of QDs/DNA complexes still stayed on the cytomembrane, some amount of the QDs/DNA complexes have been transported into the lysosome indicated with the colocalized signal of yellow. After 8 h of incubation, the red signals and green signals were overlapped very well, indicating all the complexes have been endocytosed into the lysosome and colocalized with the lysosome markers. After 24 h incubation, separate red fluorescence and green signals were clearly observed, indicating the complexes have successfully escaped from the lysosome into the cytosol, releasing the loaded DNA via the proton sponge mechanism. Therefore, the ZAIS/PEI QDs were verified as versatile self-tracking gene vectors, which could be used for insightful illustration of the gene transfection process without external labeling.[37]

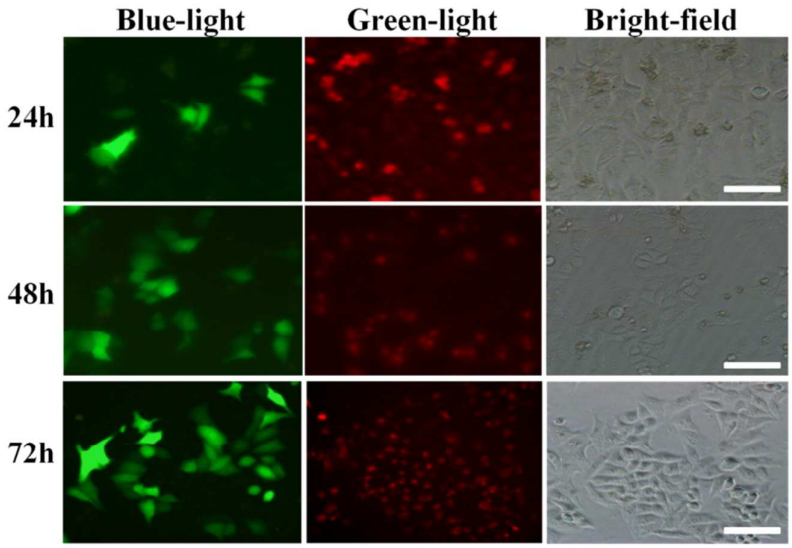

Figure 7. The fluorescence images of Hela cells at different time after transfection (The GFP was green under blue light, and the QDs were red under the green light. QDs/DNA=5/1. Scale bar: 100 μm.)

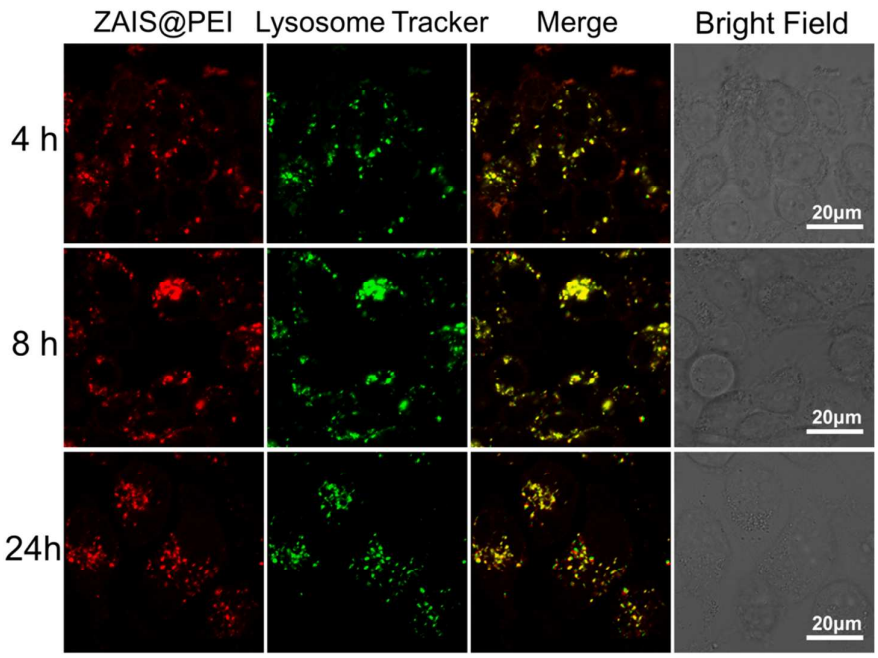

Figure 8. Time-course images of the cell internalization of the QDs/DNA complexes in Hela cells revealed by confocal microscopy. Cells were incubated with the QDs/DNA complexes at 37°C and then washed and incubated with Lysosome Tracker for 15 min, followed by further washing. The cells imaged at different time intervals. Scale bar: 20 μm.

4. Conclusions

In summary, we introduced a straightforward approach to design polycation-capped ZAIS quantum dots with integrated functions of gene delivery and bioimaging. The ZAIS@PEI QDs were water-soluble with tunable fluorescent emission ranging from 557 nm to 715 nm. The obtained ZAIS@PEI QDS vectors were able to directly condense large size of plasmid DNA into nanocomplex and efficiently transfect Hela cells with low cytotoxicity, allowing real-time monitoring gene transfection behavior

in live cells as self-tracking gene vectors without external labeling. The transfection efficiency can reach as high as 40%. It is predictable that the polycation-capped ZAIS QDs with outstanding biocompatibility possessing a great potential as a new type of gene vector.

Supporting Information

Temporal evolution of the photoluminescence and UV-absorption spectra of the ZAIS@PEI QDs (Figure S1); Full width at half maximum (FWHM) and fluorescence QY of ZAIS QDs with different Ag/In ratios (Figure S2); HRTEM image and EDX spectrogram of ZAIS@PEI QDs (Figure S3); The images under UV-light at different times after transfection (Figure S4); The images under UV-light at different times after transfection (Figure S5).

Notes：

The authors declare no competing financial interest.

Acknowledgments

The authors gratefully acknowledge the second hospital of Tianjin medical university, the National Natural Science Foundation of China (51373117, 51303126), Key Project of Tianjin Natural Science Foundation (13JCZDJC33200), National High Technology Program of China (2012AA022603) and Doctoral Base Foundation of educational Ministry of China (20120032110027).

References

1 G. Szakács，J. K. Paterson，J. A. Ludwig，C. Booth-Genthe and M. M. Gottesman, *Nat.Dev. Drug. Discov.* 2006, **5**, 219-234.

2 D. Peer，J. M. Karp，S. Hong，O. C. Farokhzad，R. Margalit and R. Langer, *Nat. Nanotechnol.* 2007, **2**, 751-760.

3 M. M. Gottesman, *Ann. Rev. Med.* 2002, **53**, 615-627.

4 Z. Wang，Z. Wang，D. Liu，X. Yan，F. Wang，G. Niu，M. Yang and X. Chen, *Angew. Chem.* 2014.

5 Z. Wang，X. Zhang，P. Huang，W. Zhao，D. Liu，L. Nie，X. Yue，S. Wang，Y. Ma and D. Kiesewetter, *Biomaterials* 2013, **34**, 6194-6201.

6 S. Nie，Y. Xing，G. J. Kim and J. W. Simons, *Annu. Rev. Biomed. Eng.* 2007, **9**, 257-288.

7 M. S. Shim and Y. J. Kwon, *Adv. Drug Deliv. Rev.* 2012, **64**, 1046-1059.

8 W. Godbey，K. K. Wu and A. G. Mikos, *J. Biomed. Mater. Res.* 1999, **45**, 268-275.

9 X. Duan，J. Xiao，Q. Yin，Z. Zhang，H. Yu，S. Mao and Y. Li, *ACS nano* 2013, **7**, 5858-5869.

10 Y. Hamanaka，T. Ogawa，M. Tsuzuki and T. Kuzuya, *J. Phys. Chem. C* 2011, **115**, 1786-1792.

11 L. Li，T. J. Daou，I. Texier，T. T. Kim Chi，N. Q. Liem and P. Reiss, *Chem. Mater.* 2009, **21**, 2422-2429.

12 T. Torimoto，M. Tada，M. Dai，T. Kameyama，S. Suzuki and S. Kuwabata, *J. Phys. Chem. C* 2012, **116**, 21895-21902.

13 T. Yatsui，F. Morigaki and T. Kawazoe, *Beilstein. J. Nanotechnol.*2014, **5**, 1767-73.

14 B. Xing，W. Li，X. Wang，H. Dou，L. Wang，K. Sun，X. He，J. Han，H. Xiao，J. Miao and Y. Li, *J. Mater. Chem.* 2010, **20**, 5664-5674.

15 J. M. Li，M. X. Zhao，H. Su，Y. Y. Wang，C. P. Tan，L. N. Ji and Z. W. Mao, *Biomaterials* 2011, **32**, 7978-7987.

16 Y. Yang，H. G. Zhu，V. L. Colvin and P. J. Alvarez, *Environ. Sci. Technol. Lett.* 2011, **45**, 4988-4994.

17 M. X. Zhao，J. M. Li，L. Y. Du，C. P. Tan，Q. Xia，Z. W. Mao and L. N. Ji, *Chem. Eur. J.* 2011, **17**, 5171-5179.

18 J. J. Zhao，X. L. Qiu，Z. P. Wang，J. Pan，J. Chen and J. S. Han, *Oncotargets and Therapy* 2013, **6**, 303-309.

19 L. Peng，M. He，B. B. Chen，Q. M. Wu，Z. L. Zhang，D. W. Pang，Y. Zhu and B. Hu, *Biomaterials* 2013, **34**, 9545-9558.

20 L. Liu，R. Hu，I. Roy，G. Lin，L. Ye，J. L. Reynolds，J. Liu，J. Liu，S. A. Schwartz and X. Zhang, *Theranostics* 2013, **3**, 109-115.

21 M. D. Regulacio，K. Y. Win，S. L. Lo，S.-Y. Zhang，X. Zhang，S. Wang，M.-Y. Han and Y. Zheng, *Nanoscale* 2013, **5**, 2322-2327.

22 R. G. Xie，X. H. Zhong and T. Basche, *Adv. Mater.* 2005, **17**, 2741-2745.

23 M. Grabolle，M. Spieles，V. Lesnyak，N. Gaponik，A. Eychmueller and U. Resch-Genger, *Anal. Chem.* 2009, **81**, 6285-6294.

24 J. Song，T. Jiang，T. Guo，L. Liu，H. Wang，T. Xia，W. Zhang，X. Ye，M. Yang，L. Zhu，R. Xia and X. Xu, *Inorg. Chem.* 2015, **54,** 1627-1633.

25 W. D. Xiang，C. P. Xie，J. Wang，J. S. Zhong，X. J. Liang，H. L. Yang，L. Luo and Z. P. Chen, *J. Alloys Compd.* 2014, **588**, 114-121.

26 B. Mao，C.-H. Chuang，F. Lu，L. Sang，J. Zhu and C. Burda, *J. Phys. Chem. C* 2013, **117**, 648-656.

27 Y. Hamanaka，T. Kuzuya，T. Sofue，T. Kino，K. Ito and K. Sumiyama, *Chem. Phys. Lett.* 2008, **466**, 176-180.

28 B. D. Mao，C. H. Chuang，C. McCleese，J. J. Zhu and C. Burda, *J. Phys. Chem. C* 2014, **118**, 13883-13889.

29 J. Q. Liu，T. Song，Q. H. Yang，J. Tan，D. H. Huang and J. Chang, *J. Mat. Chem. B* 2013, **1**, 1156-1163.

30 M. Z. Fahmi and J.-Y. Chang, *Nanoscale* 2013, **5**, 1517-1528.

31 W. S. Guo，W. T. Yang，Y. Wang，X. L. Sun，Z. Y. Liu，B. B. Zhang，J. Chang and X. Y. Chen, *Nano Res.* 2014, **7**, 1581-1591.

32 M. Chu，C. Dong，H. Zhu，X. Cai，H. Dong，T. Ren，J. Su and Y. Li, *Polym. Chem.* 2013, **4**, 2528-2539.

33 L. Feng，X. Yang，X. Shi，X. Tan，R. Peng，J. Wang and Z. Liu, *Small* 2013, **9**, 1989-1997.

34 H. Hu，X. B. Wang，S. L. Xu，W. T. Yang，F. J. Xu，J. Shen and C. Mao, *J. Mater. Chem.* 2012, **22**, 15362-15369.

35 M. P. Xiong，M. Laird Forrest，G. Ton，A. Zhao，N. M. Davies and G. S. Kwon, *Biomaterials* 2007, **28**, 4889-4900.

36 J. Liu，P. Zhang，X. Yang，K. Wang，Q. Guo，J. Huang and W. Li, *Nanotechnology* 2014, **25**. DOI: 10.1088/0957-4484/25/50/505502.

37 M. V. Yezhelyev，L. F. Qi，R. M. O'Regan，S. Nie and X. H. Gao, *J. Am. Chem. Soc.* 2008, **130**, 9006-9012.

Graphical Abstract:

Synthesis of aqueous ZAIS@PEI QDs as versatile self-tracking gene vectors, allowing real-time monitoring gene transfection behavior in live cells without external fluorescence labeling.